



# Activated carbon characterization with heterogenous kernel using CO<sub>2</sub> at high pressure

José C. A. Oliveira<sup>1</sup> · Daniel V. Gonçalves<sup>1</sup> · Pedro F.G. Silvino<sup>1</sup> · Sebastião Mardônio Pereira de Lucena<sup>1</sup>

Received: 22 February 2022 / Revised: 30 November 2022 / Accepted: 17 January 2023  
© The Author(s), under exclusive licence to Springer Science+Business Media, LLC, part of Springer Nature 2023

## Abstract

We investigated the pore size distribution obtained from adsorption isotherms kernels of CO<sub>2</sub> at 298 K on homogeneous and heterogeneous slit activated carbon models. The heterogeneous activated carbon surface was created using the reactive molecular dynamics model (rMD) which explicitly incorporates heterogeneities resulting from the oxidative etching of graphene walls. PSDs obtained with homogeneous and rMD models have been compared for different activated carbons. The rMD model resulted in an improved fit to the experimental isotherm, compared to homogeneous model. The pore size distribution obtained from CO<sub>2</sub> isotherm with rMD model systematically predicts a greater volume of ultramicropores in all activated carbons studied. Both PSDs are able to predict C1 to C4 light hydrocarbon isotherms with the rMD kernel being more accurate than the homogeneous one. The rMD model considerably reduces the discrepancies between atom-atom (AA) and unit atom (UA) molecular models of CO<sub>2</sub>. The study brings evidences that CO<sub>2</sub> at high pressures can be used to simultaneously measure the interval between ultramicropores and mesopores. Moreover, the differences between AA and UA CO<sub>2</sub> model in rMD heterogeneous ultra-micropores, limits the application of implicit heterogeneous DFT-based kernel.

**Keywords** Activated carbon · CO<sub>2</sub> adsorption · Monte Carlo simulation · Characterization

## 1 Introduction

Activated carbon remains an important nanoporous material whether in industry or science, being used in numerous technological applications. Its engineering properties are mainly determined by its ability to specifically adsorption certain fluids. The practical problem of predicting adsorption properties in activated carbons has given rise to several theoretical models capable of constructing adsorption isotherms in pore models [1]. Most studies on adsorption in the literature are limited to well-defined surfaces, such as totally homogeneous surfaces. Unfortunately, real surfaces are far from such an ideal situation, and assuming a perfect surface to study adsorption in pores can lead to discrepancies in

determining adsorption isotherms and determining textural properties [2]. Recently, the pore model obtained by reactive molecular dynamics (rMD model) was developed [3, 4], which allows a more detailed study related to structural heterogeneities in carbon materials. By applying the rMD model to obtain the PSD of activated carbons, we demonstrated that the agreement with the QSDFT method (Neimark et al. 2009) was excellent and that this model effectively condenses the average characteristics of the irregularities existing in these materials. Extending this study, we intend to verify the performance of the rMD model compared to the homogeneous model using CO<sub>2</sub> at 298 K as probe gas.

Usually, the characterization uses adsorption isotherms from N<sub>2</sub> at 77 K, being a reference to provide basic information about the structure of activated carbon. However due to the diffusivity limitations of N<sub>2</sub> at 77 K [5], it is recommended to use CO<sub>2</sub> at 273 K for better analysis of microporosity. The use of CO<sub>2</sub> at 273 K also has its experimental limitations due the difficulties of performing isotherms up to saturation pressure (34.85 bar), the usual experimental technique is limited to 1 bar, imposing a reliability window [6] to a maximum size of 15 Å [1]. For this reason, this study

✉ Sebastião Mardônio Pereira de Lucena  
lucena@ufc.br

<sup>1</sup> Department of Chemical Engineering, Laboratory of Modeling and 3D Visualization - GPSA, Universidade Federal do Ceará, Campus do Pici, Bl. 709, 60455-760 Fortaleza, CE, Brazil

**Fig. 1** (a) Homogenous slit-pore model, (b) rMD slit-pore model and (c) front view of the innermost rMD pore walls. Carbon atoms in gray

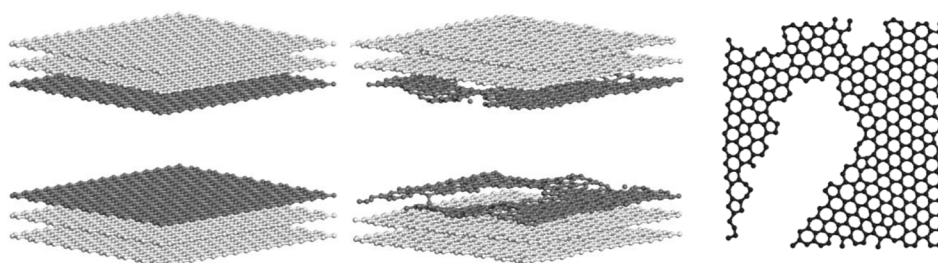


**Table 1** Fluid-fluid forcefield parameters and point charges for CO<sub>2</sub> molecules

Molecule	Model	Atom	$\sigma$ , Å	$\epsilon/k_B$ , K	$q$ , $e^-$	Distance atom-c.o.m. (Å)
CO <sub>2</sub>	Atom-Atom	United Atom	3.6485	246.15	-	-
		C	2.8	27	+0.7	0
		O	3.05	79	-0.35	1.16

will be carried out at 298 K since this isotherm is easier to obtain experimentally. The use of CO<sub>2</sub> in the characterization also has the advantages of reducing the experimental time of obtaining the isotherm, in addition to being able to test the sample under the same conditions of application, as for example for CO<sub>2</sub> capture.

In addition to the comparison with the homogeneous model, we will also investigate how heterogeneities impact the CO<sub>2</sub> molecule model. Do and collaborators [7] found that the packaging of molecular probes represented by atomic spherical model (united atom - UA) were very different from the packaging of atom-atom (AA) molecules in homogeneous slit pore models. In our previous study [4] we found that, for N<sub>2</sub> as probe gas, the heterogeneous rMD model did not present these differences identified by the Do et al. [7] study in the homogeneous model. If these differences were also negligible for CO<sub>2</sub>, it would open the possibility of adapting the QSDFT technique using the CO<sub>2</sub> unit atom model, because, due to the DFT method limitation, it is not possible to implement AA models of probe gases.

## 2 Computational methods and models

### 2.1 Reactive molecular dynamics – rMD model

Heterogeneous surfaces were used to build slit-like pores of activated carbon with different sizes. These surfaces were previously generated by simulating the oxidative etching using reactive Molecular Dynamics (rMD). Details about this procedure can be seen in our previous study [3]. In our pore model, each pore wall is composed by three layers of dimensions of 38.3 Å x 39.3 Å and interlayer space of 3.35 Å. Internal layers are heterogeneous and present 25% of carbon atoms removed while external layers are basically homogenous (Fig. 1).

### 2.2 Simulation details

Dioxide carbon adsorption isotherms at 298 K were calculated in the grand canonical ensemble using Monte Carlo method (GCMC) as implemented by the RASPA 2.0 code [8]. Biased GCMC as used in the small pores [9]. A truncated Lennard-Jones 12–6 potential without tail correction was applied. Coulomb interactions were computed using Ewald summation method. Periodic boundary conditions and a cutoff of 17 Å were utilized. For the minimum image convention to be satisfied, all simulation cells were replicated to at least 34 Å along z-axis. The pore size  $H$  used through the study, is defined as distance between the centers of carbon atoms. The effective internal pore size ( $H_{\text{eff}}$ ) used in the IUPAC Technical Report [10] is  $H_{\text{eff}} = H - \sigma_{\text{ss}}$ .

CO<sub>2</sub> molecules were modeled by single-site particles (AA model) with forcefield parameters taken from [7] and all-atom (3-site) TraPPE model [11] was also employed to investigate the influence of the model in the adsorption properties. The models accurately reproduce the vapor–liquid equilibrium data of CO<sub>2</sub> and were used in the Monte Carlo simulations (GCMC) to calculate adsorption on activated carbon [12–14]. Point charges for the all-atom model and fluid-fluid forcefield parameters for both models are presented in Table 1. The molecular parameters of carbon atom are  $\sigma_{\text{ss}} = 3.21$  Å and  $\epsilon_{\text{ss}}/k_B = 33.77$  K. The Forcefield parameters for solid-fluid interactions was applied Lorentz-Berthelot rules [15].

### 2.3 Pore size distribution

The theoretical adsorption isotherm  $\theta^{\text{theor}}$ , can be expressed as an overlap of isotherms corresponding to each pore size ( $H_j$ ), pressure  $P$  and Temperature  $T$ , which are called local isotherms,  $\theta_L$ , each with a weight corresponding to the distribution of pore size,  $f(H_j)$ :

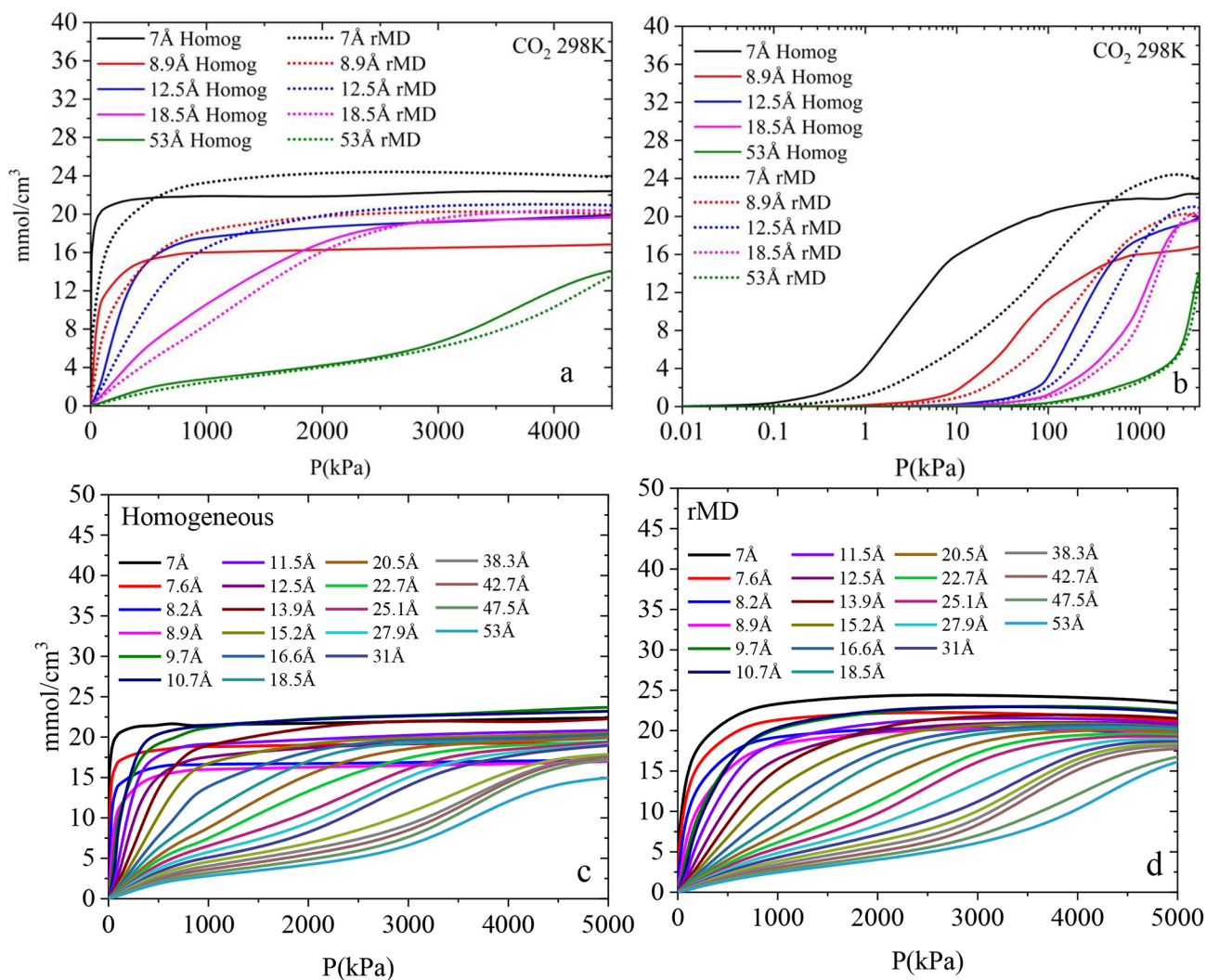


**Fig. 2** Selected simulated isotherms of CO<sub>2</sub> at 298 K with linear (a) and log (b) plot. The solid line corresponds to the homogeneous model and the dotted line corresponds to the rMD model. Complete homo-

geneous (c) and rMD (d) kernels of CO<sub>2</sub> at 298 K. Pore sizes are defined as the distance between the centers of carbon atoms

$$\theta^{theor} = \int \theta_L(H, P, T) f(H) dH \quad (1)$$

Equation 1 cannot be solved directly because it is an ill-posed equation, to minimize the problem of poor conditioning, the regularization method is used. The most commonly used method for stabilizing the result is by incorporating additional constraints that are based on smoothing the PSD [16, 17]. The pore size distribution is then derived solving (Eq. 1) numerically via a fast non-negative least square algorithm in combination with a method to stabilize the result [18, 19]. The L-curve [20] method was used to choose a regularization parameter alpha. Pore size distributions for slit pores were calculated from a kernel containing 22 pore sizes between 7Å and 53Å for CO<sub>2</sub> to 298 K.

### 3 Results and discussion

#### 3.1 Kernels of CO<sub>2</sub> adsorption isotherms with homogeneous and rMD models

In Fig. 2, simulated adsorption isotherms for CO<sub>2</sub> at 298 K are shown for some selected sizes, for homogeneous and heterogeneous (rMD) model in slit pores. The complete kernels are also shown in the Fig. 2. Three groups of behavior that were observed in methane collections of isotherms (Lastoskie et al., 1993; Lucena et al., 2010) are also present in the CO<sub>2</sub> kernel. The first group includes isotherms of pores that can accommodate only one layer of molecules. In these pores, the adsorption occurs at low pressures and the isotherm becomes flat due to the overlap of the wall potential,

with the maximum adsorption occurring at about 7 Å. The second group go approximately from 10 up to 18 Å. These are pores that accommodate two layers of molecules. When two layers are formed, the tendency of adsorption, that was decreasing as the pore dimensions increased, is reversed and causes a slight increase in adsorption at the high-pressure range. In the third group, the isotherms behavior is practically the same as the largest simulated pore (53 Å), the wall potential is weak and the cooperative effect of fluid–fluid interaction is small.

Adsorption isotherms pore filling in Fig. 2b are more abrupt when the pore is homogeneous and assumes a smooth behavior in the presence of heterogeneity. This is due to irregular packaging in the case of heterogeneous pores, compared to a much more orderly stratification in the case of homogeneous pores. The extra volume created by the cavities in the rMD model, results in greater adsorption at saturation across the micropore range. The cavities are also responsible for the delay in filling the ultramicropores that occurs in the rMD model, resulting in isotherms very different from those obtained with the homogeneous model for this size range. These differences will impact the respective pore size distributions.

### 3.2 Pore size distribution

Adsorption isotherms with CO<sub>2</sub> at high pressure are relatively rare in the literature, here, we selected a set of isotherms in order to contemplate carbons made with different raw materials and degrees of activation (Himeno et al., 2005). The simulated isotherms recovered from the pore distribution coincide very well with the experimental isotherms for the two models (homogeneous and rMD) (Fig. 3). To enable the measurement of the error, because visually, the agreement with the experimental isotherm is similar for the two models, we present the error in the form of graphs where the deviation of the theoretical adsorbed value is compared with the real value in the pressure range of the isotherm.

The WV1050 activated carbon is taken as a base case because detailed isotherms were obtained in our laboratory. This activated carbon has a surface area of 1600 m<sup>2</sup>/g, the largest among the tested activated carbons. The error graph for the WV1050 shows a better agreement for the rMD model (rMD with error of 0.068 against 0.214 for the homogenous one). The WV1050 activated carbon is also the most heterogeneous activated carbon as can be seen from the wide pore distribution proposed by the two models. For this reason, the rMD kernel better represents this activated carbon. For the other activated carbons with a narrower distribution, and therefore probably more homogeneous, with areas comprising the range of 1400 to 1150 m<sup>2</sup>/g, we

observed varied results. The BPL and A10 activated carbons show excellent agreement with the rMD model while the Norit R1 and AC-A activated carbons show less favorable agreements. In common to all analyzed activated carbons, we always observed a better agreement for the rMD model, this best agreement is systematically higher in the high-pressure intervals (> 1000 kPa).

Another common feature in the comparison with the PSD generated by the two models is the considerably greater volume attributed to ultramicropores by the rMD model (Table 2). For example, for the WV1050 the rMD model predicts twice the volume of ultramicropores (0.16 cm<sup>3</sup>/g) when compared to the homogeneous model (0.08 cm<sup>3</sup>/g). This particular fact is interesting for obtaining a PSD that covers a wide range of pores from ultramicropores that are not identified with N<sub>2</sub> at 77 K due to diffusional limitations. Currently, the identification of ultramicropores is being done with CO<sub>2</sub> at 270 K, up to 1 bar, limiting its reliability window.

We draw attention to the experimental limitations that still exist for obtaining CO<sub>2</sub> isotherms up to saturation pressures at 298 K. Due to the wide pressure range, special care must be taken in obtaining the isotherm at low pressure points up to 100 kPa. The use of specific pressure sensors for this pressure range are essential for detailing this region of the isotherm.

### 3.3 Retrieving isotherms of other gases

Another method to measure the accuracy of models is to analyze the PSD's ability to predict the adsorption of other gases. As we performed detailed experimental isotherms with light hydrocarbon (C1 to C4) for the WV1050 activated carbon, we calculated their simulated isotherms based on the CO<sub>2</sub> PSDs of the homogenous and rMD models using the representative pore methodology (Oliveira et al. 2021). This same calculation was done previously using a kernel of pores representative of N<sub>2</sub> at 77 K [21]. The result can be seen in Fig. 4. The experimental isotherms are recovered with both PSDs, with the rMD model always showing better fitting than the homogeneous model. This result is important because one of the advantages of using molecular simulation methods is to obtain detailed isotherms of mixtures that are difficult to perform experimentally.

### 3.4 Impact of the probe-gas model

As previously commented, Do et al. [7] showed that the unit atom model cannot adequately describe CO<sub>2</sub> adsorption in slit pores. For the 6.5 Å (center to center) pore at 193 K this discrepancy is visible as shown in Fig. 5a and b. These figures were obtained from the simulation of AA

**Fig. 3** PSDs for activated carbons (a) WV1050 (b) BPL (c) A10 (d) Norit R1 and (e) AC-A calculated using kernels based in rMD and homogeneous model. The inset graphs present the fitting of experimental and simulated CO<sub>2</sub> adsorption isotherms at 298 K. In the right column the absolute error of fitting of experimental adsorption isotherms. Blue bars and lines: rMD model. Red bars and lines: Homogeneous model. Pore sizes are defined as the distance between the centers of carbon atoms

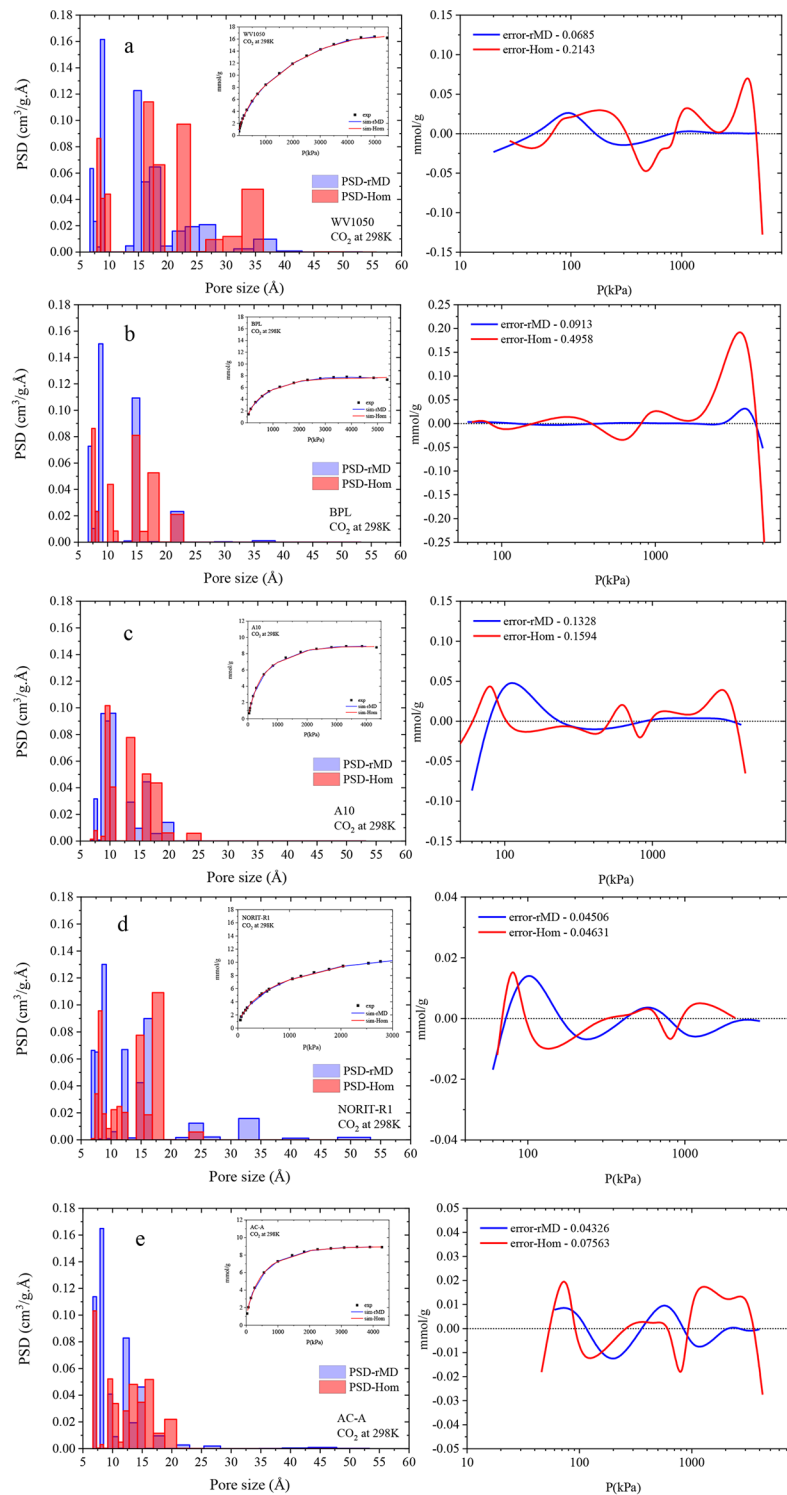


**Table 2** Pore volume of ultramicropore, supermicropore, mesopore and total volume attributed for the activated carbons investigated

	rMD	Homog.	rMD	Homog.	rMD	Homog.	rMD	Homog.	rMD	Homog.
Ultramicropore	0.1674	0.0803	0.1691	0.0657	0.087	0.0081	0.1702	0.0919	0.1672	0.0642
Supermicropore	0.4079	0.5353	0.1961	0.3136	0.3225	0.3965	0.2607	0.4035	0.2366	0.3593
Mesopore	0.159	0.2265	0.0055	0.0001	0.011	0.0143	0.1047	0.0141	0.0134	0.0003
V <sub>total</sub>	0.7313	0.8421	0.3707	0.3795	0.4103	0.4185	0.5355	0.5095	0.4172	0.4238



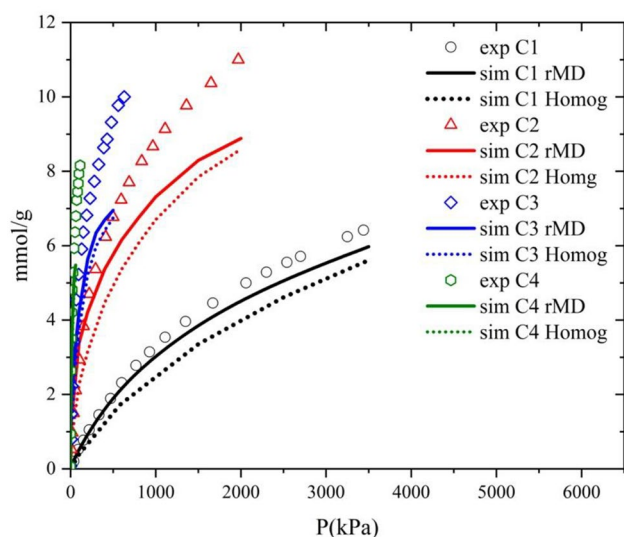


**Fig. 4** Experimental (symbol) and simulated (lines) adsorption isotherms at 298 K of C1, C2, C3 and C4, on WV-1050 using rMD and homogeneous PSDs. Full line – rMD model. Dotted line – homogeneous model

and UA models in homogeneous pores. Figure 5a shows the results obtained by Do while Fig. 5b shows the results of our simulation with our homogeneous pore model. The greatest discrepancy between UA and AA models in the 6.5 Å homogeneous pore is related to the one-layer limit for the gas adsorption in the pore. While the CO<sub>2</sub> UA molecules do not show any particular orientation, the AA molecules assume a preferential orientation, positioning parallel to the surface compromise the packaging and the fluid-fluid interaction. Unlike N<sub>2</sub>, in the case of CO<sub>2</sub>, this difference is greater and more persistent.

In our previous study [4], we showed that when using the rMD model, this difference between the gas models practically disappears for N<sub>2</sub> molecules. To test the behavior of CO<sub>2</sub>, we performed a similar test with the AA and UA models of CO<sub>2</sub>. Due to the heterogeneity present in the innermost pore wall of the rMD model, the effect of the molecule geometry is attenuated (Fig. 5c), the volume accessible to the molecule is irregular allowing a greater degree of freedom for the organization within the pore, establishing multiples adsorption zones and preventing preferential orientation.

This result points to the possibility of using implicit heterogeneous models such as QSDFT or 2D NLDFT (Jagiello and Jaroniec 2018) in the elaboration of kernels based on CO<sub>2</sub> isotherms up to saturation pressure. We know that due to limitations of DFT-based methods, heterogeneous gas models cannot be implemented. However, as the difference is reduced on heterogeneous surfaces, the model can be used as a good approximation.

## 4 Conclusion

We examined the performance of a heterogeneous kernel of CO<sub>2</sub> at 298 K, obtained by reactive molecular dynamics (rMD model), in predicting the pore distribution of a series of activated carbons compared to a homogeneous kernel. As the agreement of the two kernels are visually good, we measure the errors from the deviation of the absolute values in the pressure range of the isotherms. From the error analysis, it is evident that the rMD model is more accurate in the recovery of experimental isotherms, systematically presenting a greater volume of ultramicropores than the homogeneous model. The pore distributions of the two kernels were also able to predict the adsorption of light hydrocarbons (C1 to C4), where again, the rMD model presents better results than the homogeneous one. Finally, we tested the impact of the heterogeneous surface for AA and UA molecular models of CO<sub>2</sub>. Unlike the homogeneous model, the discrepancies between the molecular models of the gas are considerably reduced for the rMD model.

We believe that this set of results may enable the use of CO<sub>2</sub> to analyze, in a single experimental run, from ultramicropores to mesopores with a maximum value of 50 Å. The fact that the CO<sub>2</sub> PSD is capable of predicting adsorption of other gases is of significant importance in the design of materials in industrial processes because the prediction of multicomponent adsorption on activated carbons becomes feasible. Finally, the discrepancy between the gas models (AA and UA), when using a heterogeneous surface, are still significant for the case of CO<sub>2</sub> as adsorbent in the ultramicropore range. This limitation imposes a restriction on the use of DFT-based methods in the elaboration of kernels using CO<sub>2</sub> as a probe gas.

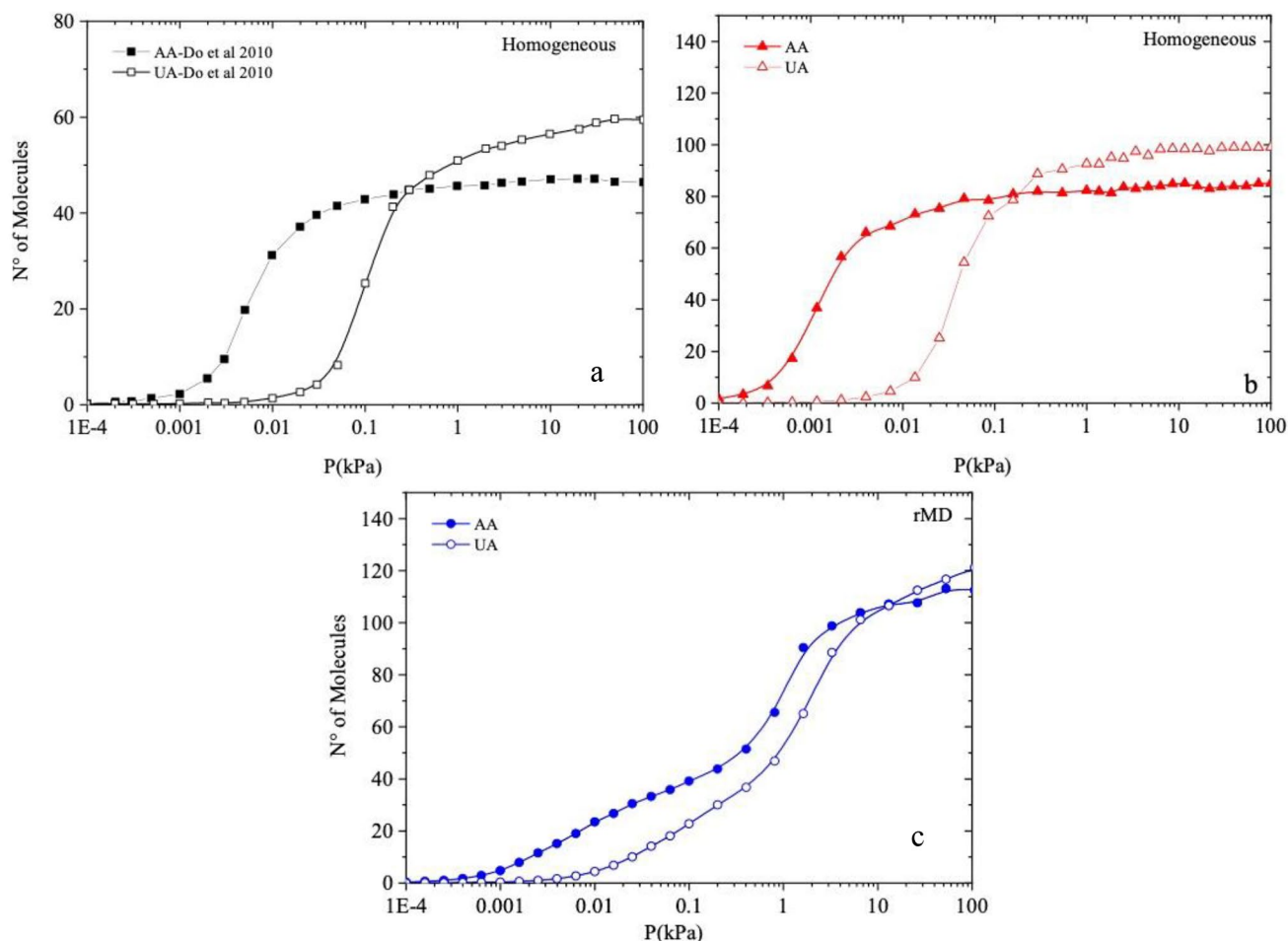


**Fig. 5** AA and UA CO<sub>2</sub> adsorption isotherm at 193 K on 6.5 Å (center to center) pore using homogeneous (a) Do et al. [7] results and (b) our results and (c) rMD pore models. The AA CO<sub>2</sub> model is shown

**Acknowledgement** The authors wish to acknowledge financial support for this study from CAPES, CNPq and FUNCAP and the use of the computer cluster at National Laboratory of Scientific Computing (LNCC/MCTI, Brazil).

## Declarations

**Conflict of interest** The authors have no competing interests to declare that are relevant to the content of this article.

## References

- Ravikovitch, P.I., Vishnyakov, A., Russo, R., Neimark, A.V.: Unified Approach to pore size characterization of Microporous Carbonaceous materials from N<sub>2</sub>, Ar, and CO<sub>2</sub> Adsorption Isotherms. *Langmuir*. **16**, 2311–2320 (2000). <https://doi.org/10.1021/la991011c>
- Do, D.D., Do, H.D.: Effects of potential models on the adsorption of carbon dioxide on graphitized thermal carbon black: GCMC computer simulations. *Colloids Surf. Physicochem Eng Asp*. **277**, 239–248 (2006). <https://doi.org/10.1016/j.colsurfa.2005.11.094>
- Lucena, S.M.P., Gonçalves, R.V., Silvino, P.F.G., Gonçalves, D.V., Oliveira, J.C.A.: Fingerprints of heterogeneities from carbon oxidative process: a reactive molecular dynamics study. *Microporous Mesoporous Mater.* **304**, 109061 (2020). <https://doi.org/10.1016/j.micromeso.2018.07.051>
- Lucena, S.M.P., Oliveira, J.C.A., Gonçalves, D.V., Silvino, P.F.G., Dantas, S., Neimark, A.V.: Pore size analysis of carbons with heterogeneous kernels from reactive molecular dynamics model and quenched solid density functional theory. *Carbon N. Y.* **183**, 672–684 (2021). <https://doi.org/10.1016/j.carbon.2021.07.059>
- Jagiello, J., Ania, C., Parra, J.B., Cook, C.: Dual gas analysis of microporous carbons using 2D-NLDFT heterogeneous surface model and combined adsorption data of N<sub>2</sub> and CO<sub>2</sub>. *Carbon N. Y.* **91**, 330–337 (2015). <https://doi.org/10.1016/j.carbon.2015.05.004>
- Gusev, V.Y., O'Brien, J., Seaton, N.A., Brien, J.A.O.: A self-consistent method for characterization of activated carbons using supercritical adsorption and Grand Canonical Monte Carlo Simulations. *Langmuir*. **13**, 2815–2821 (1997). <https://doi.org/10.1021/la960421n>
- Do, D.D.D., Junpirom, S., Nicholson, D., Do, H.D.D.: Importance of molecular shape in the adsorption of nitrogen, carbon dioxide and methane on surfaces and in confined spaces. *Colloids*

- Surf. Physicochem Eng Asp. **353**, 10–29 (2010). <https://doi.org/10.1016/j.colsurfa.2009.10.021>
8. Dubbeldam, D., Calero, S., Ellis, D.E., Snurr, R.Q.: RASPA: molecular simulation software for adsorption and diffusion in flexible nanoporous materials. *Mol. Simul.* **42**, 81–101 (2016). <https://doi.org/10.1080/08927022.2015.1010082>
  9. Lucena, S.M.P., Snurr, R.Q., Cavalcante, C.L.: Studies on adsorption equilibrium of xylenes in AEL framework using biased GCMC and energy minimization. *Microporous Mesoporous Mater.* **111**, 89–96 (2008). <https://doi.org/10.1016/j.micromeso.2007.07.021>
  10. Thommes, M., Kaneko, K., Neimark, A.V., Olivier, J.P., Rodriguez-Reinoso, F., Rouquerol, J., Sing, K.S.W.: Physisorption of gases, with special reference to the evaluation of surface area and pore size distribution (IUPAC Technical Report). *Pure Appl. Chem.* **87**, 1051–1069 (2015)
  11. Potoff, J.J., Siepmann, J.I.: Vapor–liquid equilibria of mixtures containing alkanes, carbon dioxide, and nitrogen. *AIChE J.* **47**, 1676–1682 (2001). <https://doi.org/10.1002/aic.690470719>
  12. Dantas, S., Struckhoff, K.C., Thommes, M., Neimark, A.V.: Pore size characterization of micro-mesoporous carbons using CO<sub>2</sub> adsorption. *Carbon N. Y.* **173**, 842–848 (2021). <https://doi.org/10.1016/j.carbon.2020.11.059>
  13. Gonçalves, D.V., Paiva, M.A.G., Oliveira, J.C.A., Bastos-Neto, M., Lucena, S.M.P.: Prediction of the monocomponent adsorption of H<sub>2</sub>S and mixtures with CO<sub>2</sub> and CH<sub>4</sub> on activated carbons. *Colloids Surf. Physicochem Eng Asp.* **559**, 342–350 (2018). <https://doi.org/10.1016/j.colsurfa.2018.09.082>
  14. Soares Maia, D.A., Alexandre de Oliveira, J.C., Nazzarro, M.S., Sapag, K.M., López, R.H., de Lucena, S.M.P., de Azevedo, D.C.S.: CO<sub>2</sub> gas-adsorption calorimetry applied to the study of chemically activated carbons. *Chem. Eng. Res. Des.* **136**, 753–760 (2018). <https://doi.org/10.1016/j.cherd.2018.06.034>
  15. Steele, W.A.: The interaction of rare gas atoms with graphitized carbon black. *J. Phys. Chem.* **82**, 817–821 (1978). <https://doi.org/10.1021/j100496a011>
  16. Merz, P.H.: Determination of adsorption energy distribution by regularization and a characterization of certain adsorption isotherms. *J. Comput. Phys.* **38**, 64–85 (1980). [https://doi.org/10.1016/0021-9991\(80\)90012-1](https://doi.org/10.1016/0021-9991(80)90012-1)
  17. Szombathely, M.V., Bräuer, P., Jaroniec, M.: The solution of adsorption integral equations by means of the regularization method. *J. Comput. Chem.* **13**, 17–32 (1992). <https://doi.org/10.1002/jcc.540130104>
  18. Davies, G.M., Seaton, N.: Development and validation of pore structure models for activated carbons. *Langmuir.* **15**, 6263 (1999). <https://doi.org/10.1021/la990160s>
  19. Davies, G.M., Seaton, N.A.: The effect of the choice of pore model on the characterization of the internal structure of microporous carbons using pore size distributions. *Carbon N. Y.* **36**, 1473–1490 [https://doi.org/S0008-6223\(98\)00140-7](https://doi.org/S0008-6223(98)00140-7) (1998)
  20. Hansen, P.C.: Regularization Tools: A Matlab package for analysis and solution of discrete ill-posed problems. *Numer. Algorithms.* **6**, (1994)
  21. Lucena, S.M.P., Gomes, V., Gonçalves, D.V., Mileo, P.G.M., Silvino, P.F.G.: Molecular simulation of the accumulation of alkanes from natural gas in carbonaceous materials. *Carbon N. Y.* **61**, 624–632 (2013). <https://doi.org/10.1016/j.carbon.2013.05.046>

**Publisher's Note** Springer Nature remains neutral with regard to jurisdictional claims in published maps and institutional affiliations.

Springer Nature or its licensor (e.g. a society or other partner) holds exclusive rights to this article under a publishing agreement with the author(s) or other rightsholder(s); author self-archiving of the accepted manuscript version of this article is solely governed by the terms of such publishing agreement and applicable law.



## Terms and Conditions

Springer Nature journal content, brought to you courtesy of Springer Nature Customer Service Center GmbH (“Springer Nature”).

Springer Nature supports a reasonable amount of sharing of research papers by authors, subscribers and authorised users (“Users”), for small-scale personal, non-commercial use provided that all copyright, trade and service marks and other proprietary notices are maintained. By accessing, sharing, receiving or otherwise using the Springer Nature journal content you agree to these terms of use (“Terms”). For these purposes, Springer Nature considers academic use (by researchers and students) to be non-commercial.

These Terms are supplementary and will apply in addition to any applicable website terms and conditions, a relevant site licence or a personal subscription. These Terms will prevail over any conflict or ambiguity with regards to the relevant terms, a site licence or a personal subscription (to the extent of the conflict or ambiguity only). For Creative Commons-licensed articles, the terms of the Creative Commons license used will apply.

We collect and use personal data to provide access to the Springer Nature journal content. We may also use these personal data internally within ResearchGate and Springer Nature and as agreed share it, in an anonymised way, for purposes of tracking, analysis and reporting. We will not otherwise disclose your personal data outside the ResearchGate or the Springer Nature group of companies unless we have your permission as detailed in the Privacy Policy.

While Users may use the Springer Nature journal content for small scale, personal non-commercial use, it is important to note that Users may not:

1. use such content for the purpose of providing other users with access on a regular or large scale basis or as a means to circumvent access control;
2. use such content where to do so would be considered a criminal or statutory offence in any jurisdiction, or gives rise to civil liability, or is otherwise unlawful;
3. falsely or misleadingly imply or suggest endorsement, approval, sponsorship, or association unless explicitly agreed to by Springer Nature in writing;
4. use bots or other automated methods to access the content or redirect messages
5. override any security feature or exclusionary protocol; or
6. share the content in order to create substitute for Springer Nature products or services or a systematic database of Springer Nature journal content.

In line with the restriction against commercial use, Springer Nature does not permit the creation of a product or service that creates revenue, royalties, rent or income from our content or its inclusion as part of a paid for service or for other commercial gain. Springer Nature journal content cannot be used for inter-library loans and librarians may not upload Springer Nature journal content on a large scale into their, or any other, institutional repository.

These terms of use are reviewed regularly and may be amended at any time. Springer Nature is not obligated to publish any information or content on this website and may remove it or features or functionality at our sole discretion, at any time with or without notice. Springer Nature may revoke this licence to you at any time and remove access to any copies of the Springer Nature journal content which have been saved.

To the fullest extent permitted by law, Springer Nature makes no warranties, representations or guarantees to Users, either express or implied with respect to the Springer nature journal content and all parties disclaim and waive any implied warranties or warranties imposed by law, including merchantability or fitness for any particular purpose.

Please note that these rights do not automatically extend to content, data or other material published by Springer Nature that may be licensed from third parties.

If you would like to use or distribute our Springer Nature journal content to a wider audience or on a regular basis or in any other manner not expressly permitted by these Terms, please contact Springer Nature at

[onlineservice@springernature.com](mailto:onlineservice@springernature.com)